# Indoor MIMO Visible Light Communications: Novel Angle Diversity Receivers for Mobile Users

Asanka Nuwanpriya, Ho Siu-Wai, Chung Shue Chen

# Indoor MIMO Visible Light Communications: Novel Angle Diversity Receivers for Mobile Users

Asanka Nuwanpriya, *Student Member, IEEE*, Siu-Wai Ho, *Senior Member, IEEE*, and Chung Shue Chen, *Member, IEEE*

***Abstract*—This paper proposes two novel and practical designs of angle diversity receivers to achieve multiple-input-multiple-output (MIMO) capacity for indoor visible light communications (VLC). Both designs are easy to be constructed and suitable for small mobile devices. By using light emitting diodes for both illumination and data transmission, our receiver designs consist of multiple photodetectors (PDs) which are oriented with different inclination angles to achieve high-rank MIMO channels and can be closely packed without the requirement of spatial separation. Due to the orientations of the PDs, the proposed receiver designs are named pyramid receiver (PR) and hemispheric receiver (HR). In a PR, the normal vectors of PDs are chosen the same as the normal vectors of the triangle faces of a pyramid with equilateral $N$-gon base. On the other hand, the idea of HR is to evenly distribute the PDs on a hemisphere. Through analytical investigation, simulations and experiments, the channel capacity and bit-error-rate (BER) performance under various settings are presented to show that our receiver designs are practical and promising for enabling VLC-MIMO. In comparison to induced link-blocked receiver, our designs do not require any hardware adjustment at the receiver from location to location so that they can support user mobility. Besides, their channel capacities and BER performance are quite close to that of link-blocked receiver. Meanwhile, they substantially outperform spatially-separated receiver. This study reveals that using angle diversity to build VLC-MIMO system is very promising.**

***Index Terms*—Visible light communications, multiple-input-multiple-output (MIMO), angle diversity, pyramid receiver, hemispheric receiver.**

## I. Introduction

OPTICAL wireless communications (OWC) is a promising communications technology, which has garnered a lot of interest since the pioneering work of Gfeller and Bapst [1] and recently raises many inspiring discussions for its new potential in future wireless systems [2]. Using emerging illumination devices white light emitting diodes (LEDs) as transmitters, visible light communications (VLC) has been a fast growing OWC technology and gained much attention in the last few years, in particular indoor optical wireless communications (see e.g., [3–5]). The advancement of solid-state lighting technology and the benefit of simultaneous illumination and data communications have seen VLC systems rapidly evolving as a viable and attractive communications technology [6]. Besides, VLC uses the visible light spectrum which is unregulated and license-free and more importantly it does not interfere with existing radio frequency (RF) systems.

Although the available optical bandwidth for VLC is around $400$ THz, the electrical bandwidth is limited to several MHz by white LED transmitters [7]. Therefore, to achieve high data rates, it is vital to employ highly spectral-efficient techniques such as orthogonal frequency division multiplexing (OFDM) and multiple-input-multiple-output (MIMO). In an indoor VLC system, usually there are several LED sources illuminating the area and hence it is natural to use MIMO technique to have parallel data transmission or spatial multiplexing (SM) to increase the data rate (see e.g., [4, 8]). However, for indoor VLC systems with direct line-of-sight (LoS), the MIMO channel matrix can be highly correlated, which prevents successful decoding of the parallel channels in the receiver [9, 10].

There are various methods described in literature to reduce channel correlation. A receiver with imaging lens and a detector array is considered in [8] while spatial separation between receiver photodetectors (PDs), power imbalance among transmitters and link blockage are considered in [11]. Imaging lens with a detector array is non-trivial to be constructed and the size of the array can be large [8, 12]. Power imbalance among transmitters can sometimes reduce channel correlation but not always. Link-blocked (LB) receiver is found to be a more suitable method to achieve a good channel performance [11] when the receiver is static at a location. A link-blocked receiver however involves using an opaque boundary to block a particular link from a LED to a PD. Therefore, it would not be easy to use this technique for high-mobility applications. It might be further practically difficult to block a particular link when the spatial separation between each PD is required to be small. On the other hand, a receiver array with spatially separated PDs is a practically implementable and can support mobility as shown in [11]. We call it spatially separated (SS) receiver in this paper.

In this paper, we propose an alternative to achieve highly uncorrelated VLC-MIMO channels by varying the orientation angles of the PDs. A similar method was proposed in [5][13] to improve the coverage of optical wireless systems by angle diversity so that full mobility can be supported and signal blocking can be avoided. To the best of our knowledge, we were the first to consider achieving multiplexing gain by angle diversity [14]. In this paper, we extend our work and provide

Manuscript received June 07, 2014; revised November 10, 2014 and March 20, 2015; accepted April 12, 2015.

A part of the work was presented at the IEEE Global Communications Conference (Globecom 2014) Workshop on Optical Wireless Communications in Austin, USA.

Asanka Nuwanpriya and Siu-Wai Ho are with Institute for Telecommunications Research, University of South Australia, Australia (e-mail: kekay001@mymail.unisa.edu.au; siuwai.ho@unisa.edu.au).

Chung Shue Chen is with Alcatel-Lucent Bell Labs, Centre de Villarceaux, 91620 Nozay, France (e-mail: cs.chen@alcatel-lucent.com). A part of the work of C. S. Chen presented in this paper was carried out at LINCS (www.lincs.fr).

details of practical design aspects of angle diversity receivers for VLC-MIMO and their performance analysis, considering both the achievable capacity and bit-error-rate (BER). In this paper, we propose two new designs of PD array, namely *pyramid* receiver (PR) and *hemispheric* receiver (HR), and find their optimal system parameters, especially the optimal angles of the orientation of PDs. We also consider their achievable capacities at different indoor locations.

The proposed receivers are compared with other receiver designs including SS receiver and LB receiver [11]. Results show that the two proposed receiver designs have good performance in both the channel capacity (see Section IV) and BER (see Section VI) and are practical solutions to enable VLC-MIMO transmission. Meanwhile, they can substantially outperform SS receiver. Note that both the PR and HR can be easily constructed in a receiver with small size which is especially desirable for today's hand-held or mobile devices.

The rest of the paper is organized as follows. Section II describes the system model, proposed receiver designs, and analytical channel capacity. Section III presents the framework of theoretical evaluation for BER and discusses the possible effect of the PD field of view characteristics on the channel capacity. Numerical evaluations are carried out in Section IV to compare the channel capacities of various receivers including link-blocked and spatially separated receivers. Section VI compares the BER performance of different receiver designs. Section VII uses experiments to verify our simulation and analytical results and completes the comparative studies. Finally, we will discuss the future work in Section VIII before Section IX concludes the paper.

*Notation:* $(.)^T$ and $(.)^*$ denote transpose and conjugate (Hermitian) transpose, respectively.

## II. System Model and Proposed Receivers

We first explain the VLC-MIMO system model and then present the proposed receiver designs in detail.

### A. System Model

Consider an optical wireless MIMO system with $M$ white LED transmitters and $N$ PD receivers. Intensity modulation (IM) and direct detection (DD) are the optical modulation and demodulation schemes. The shot and thermal noises in the receiver are modeled as additive white Gaussian noise (AWGN) and are added to the signal in the electrical domain [11]. The links are assumed to have direct LoS and reflections are not considered.

At first the binary transmit signal is modulated. Unipolar $K$-PAM (pulse amplitude modulation) is considered as the electrical modulation, where the $i$-th modulated signal is denoted by $x_i \in [0, \cdots, (K-1)]$, where $K$ is the modulation size. This modulated transmit signal is parsed into a vector of length $M$, denoted by $\mathbf{x} = [x_0, x_1, \cdots, x_{M-1}]^T$. The received vector of length $N$ can be written as

$$\mathbf{y} = \mathbf{H}\mathbf{x} + \mathbf{w}, \tag{1}$$

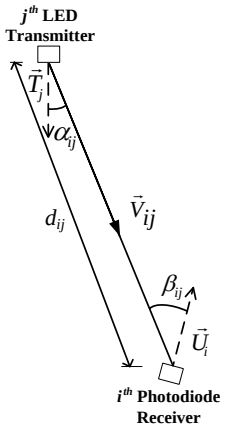


Fig. 1: The geometry of a transmitter-receiver pair.

where $\mathbf{w} = [w_0, w_1, \cdots, w_{N-1}]^T$ denotes independent identically distributed (i.i.d.) AWGN samples with $w_i \sim \mathcal{N}(0, N_o/2)$, where $N_o$ is the single sided noise power spectral density [15]. The total noise variance $\sigma_n^2 = N_o/2 = \sigma_{\text{shot}}^2 + \sigma_{\text{thermal}}^2$, where $\sigma_{\text{shot}}^2$ is the shot noise variance and $\sigma_{\text{thermal}}^2$ is the thermal noise variance [11] and $\mathbf{H}$ is the $N \times M$ channel matrix given by

$$\mathbf{H} = \begin{pmatrix} h_{11} & \cdots & h_{1M} \\ \vdots & \ddots & \vdots \\ h_{N1} & \cdots & h_{NM} \end{pmatrix}, \tag{2}$$

where $h_{ij}$ represents the MIMO channel gain between transmitter $j$ and receiver $i$. For a transmitter and receiver pair as shown in Fig. 1, $h_{ij}$ can be found by

$$h_{ij} = \frac{(m+1)A}{2\pi d_{ij}^2} \cos^m(\alpha_{ij}) \cos^k(\beta_{ij}) \tag{3}$$

if $-\frac{\pi}{2} \le \alpha_{ij} \le \frac{\pi}{2}$ and $-\frac{\pi}{2} \le \beta_{ij} \le \frac{\pi}{2}$. Otherwise, $h_{ij} = 0$. The Lambertian emission order is given in (3) as

$$m = \frac{-\ln 2}{\ln(\cos \Phi_{1/2})},$$

where $\Phi_{1/2}$ is the LED semi-angle at half-power. In (3), $A$ is the active area of the PD, and $k$ is the field-of-view (FoV) coefficient of the PD receiver [16].

Here, $\alpha_{ij}$, $\beta_{ij}$ and $d_{ij}$ are the irradiance angle at LED $i$ with respect to PD $j$, the incident angle at PD $j$ with respect to LED $i$, and the distance between LED $i$ and PD $j$, respectively. There are three vectors of interest for a particular link between an LED and a PD, which are depicted in Fig. 1:

- $\overrightarrow{T_j}$: the normal vector of the LED $j$ in the direction of irradiance,
- $\overrightarrow{V_{ij}}$: the vector from the LED $j$ to the PD $i$, and
- $\overrightarrow{U_i}$: the normal vector of the PD $i$ in the direction of incident light.

From these vectors, we can find $\alpha_{ij}$ and $\beta_{ij}$ using vector dot

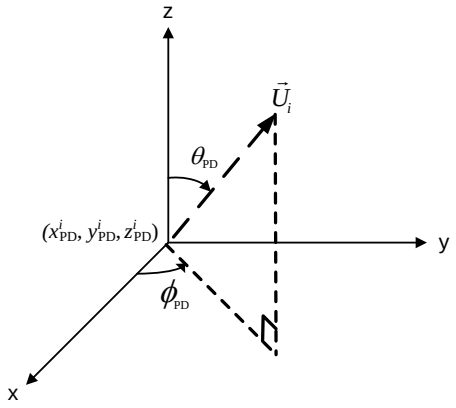


Fig. 2: The coordinate system.

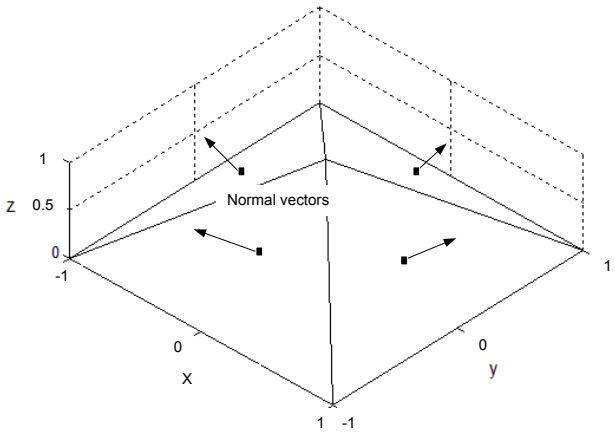


Fig. 3: In PR, the normal vectors of PDs are chosen according to the normal vectors on the surfaces of a pyramid for $N = 4$.

product as follows:

$$\cos(\alpha_{ij}) = \frac{\overrightarrow{T_j} \cdot \overrightarrow{V_{ij}}}{||\overrightarrow{T_j}|| \; ||\overrightarrow{V_{ij}}||}, \quad (4)$$

$$\cos(\beta_{ij}) = \frac{\overrightarrow{V_{ji}} \cdot \overrightarrow{U_i}}{||\overrightarrow{V_{ji}}|| \; ||\overrightarrow{U_i}||}. \quad (5)$$

The estimated received vector $\hat{\mathbf{x}}$ of length $N$ can be calculated as

$$\hat{\mathbf{x}} = \mathbf{Eq_{ZF}}\, \mathbf{y}, \quad (6)$$

where $\mathbf{Eq_{ZF}} \triangleq (\mathbf{H}^*\mathbf{H})^{-1}\mathbf{H}^*$ is the zero-forcing equalizer. Electrical demodulation is performed on $\hat{\mathbf{x}}$ to construct the estimate of the received information data.

Here we consider that the receiver knows the channel statistics but the transmitter does not, i.e., channel side information at receiver (CSI-R) scenario. Therefore, equal power is allocated to each transmit antenna and the channel capacity of the MIMO system is given by [17]

$$C_{\text{EP}} = \sum_{i}^{R_H} \log_2 \left[1 + \frac{\text{SNR}_{\text{elec}}}{M} \lambda_i\right], \quad (7)$$

where $\text{SNR}_{\text{elec}} \triangleq P_{\text{elec}}/N_o$ is the average electrical SNR per transmit antenna, $P_{\text{elec}}$ is the transmit power constraint of the system, $\lambda_i$ is the $i$-th eigenvalue of $\mathbf{HH}^*$, and $R_H$ is the number of non-zero singular values of $\mathbf{H}$. We will use (7) as a benchmark to compare our proposed systems.

We can see from (6) that in order to successfully receive the transmit signal, the channel matrix $\mathbf{H}$ has to be full rank. Correlation between the wireless channel links may cause the channel matrix non-invertible and hence should be avoided in a MIMO system.

### B. Coordinate System

The positions and the orientations of the LEDs and PDs are specified by their normal vectors in $[x, y, z, \phi, \theta]$ format, where $(x, y, z)$ are the Cartesian coordinates of the originating position of a vector, and $\theta \in [0, \pi]$ and $\phi \in [0, 2\pi]$ are the angles from the positive $z$-axis (i.e., the elevation angle) and the positive $x$-axis (i.e., the azimuth angle), respectively. An example is shown in Fig. 2 where the normal vector $\overrightarrow{U_i}$ of PD $i$ is specified by $[x^i_{\text{PD}}, y^i_{\text{PD}}, z^i_{\text{PD}}, \phi_{\text{PD}}, \theta_{\text{PD}}]$.

In the following, a transmitter LED $j$ placed at $(x^j_{\text{LED}}, y^j_{\text{LED}}, z^j_{\text{LED}})$ has its normal vector $\overrightarrow{T_j}$ specified by $[x^j_{\text{LED}}, y^j_{\text{LED}}, z^j_{\text{LED}}, \phi^j_{\text{LED}}, \theta^j_{\text{LED}}]$, for $1 \le j \le M$. Similarly, a receiver PD $i$ placed at $(x^i_{\text{PD}}, y^i_{\text{PD}}, z^i_{\text{PD}})$ has its normal vector $\overrightarrow{U_i}$ given by $[x^i_{\text{PD}}, y^i_{\text{PD}}, z^i_{\text{PD}}, \phi^i_{\text{PD}}, \theta^i_{\text{PD}}]$, for $1 \le i \le N$.

### C. Proposed Receivers

Here we introduce the proposed receiver designs, which are simple and practically feasible. For both receivers, the PDs are always located on a small horizontal plane so that the receiver size is small. As a result, the distances between the PDs and the same LED are nearly the same. This is especially true when the distance between the LED and the receiver is much larger than the separation between the PDs in a receiver. In order to have highly uncorrelated channel gains, the main idea of our receiver design is to vary the normal vector of each PD such that the incident angles from the same LED are different. There are however numerous ways of choosing the orientation of the normal vectors. In this paper, we will focus on two receiver designs: 1) the pyramid receiver (PR), and 2) the hemispheric receiver (HR). In a nutshell, we consider some points on the surface of a pyramid (or a hemisphere) to determine the normal vectors of the PDs in a PR (or a HR). For example, consider a pyramid with a square base as shown in Fig. 3. The normal vectors on the surfaces of the pyramid are used to define the normal vectors of PDs in a PR. As a result, the PDs are pointing to different directions. On the other hand, to construct a HR, we first evenly distribute $N$ points on the surface of a unit hemisphere as depicted in Fig. 4 such that the normal vector of each point is pointing to a different direction. We will then use the orientation of these normal vectors to define the normal vectors of the PDs in a HR. Note that Fig. 3 and Fig. 4 are only used to demonstrate how the normal vectors of the PDs in a receiver are chosen.

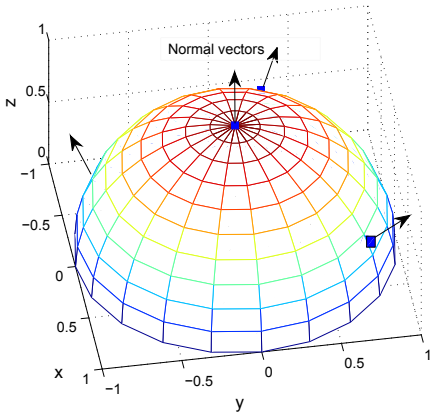


Fig. 4: In HR, the normal vectors of PDs are chosen according to the normal vectors on $N$ different positions on the surface of a hemisphere for $N = 4$.

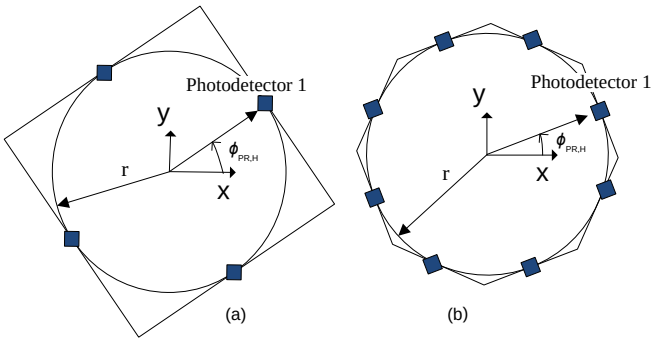


Fig. 5: PD arrangement of PR (and HR) on the horizontal plane (x-y plane) for (a) $N = 4$ and (b) $N = 8$. The squares indicate the locations of the PDs. The normal vectors of PDs in (a) are chosen according to Fig. 3 and Fig. 4 for PR and HR, respectively.

When we formally define PR and HR later in Sections II-C.1 and II-C.2, the PDs are always located on a horizontal plane.

Note that the structures of both the PR and HR are especially suitable for hand-held devices such as smart-phones, tablet devices or small mobile devices because the spatial separation between the PDs is not necessary and the receiver can thus be very compact. We will discuss this point later in Fig. 6 and Fig. 7, which illustrate the top and side views of PR and HR, respectively, constructed using four typical off-the-shelf PDs. It is clear that the diversity gain can be further improved if a flexibility of spatial separation is granted given a larger receiver size. However, this is outside the scope of this paper.

*1) Definition of Pyramid Receiver (PR):* The receiver is called a pyramid receiver because the PDs on it are pointing to different directions just like the triangle faces (except the base) of a pyramid. However, it is not necessary that the receiver must look like a pyramid. The rigorous definition of a PR is detailed below.

The PDs are arranged uniformly in a circle of radius $r$ on the horizontal plane. For $1 \leq i \leq N$, the coordinates of PD $i$ are given by

$$(x^i_{\text{PD}}, y^i_{\text{PD}}, z^i_{\text{PD}}) = \left(x_{\text{PD}} + r\cos\frac{2(i-1)\pi}{N}, y_{\text{PD}} + r\sin\frac{2(i-1)\pi}{N}, h_{\text{PD}}\right), \quad (8)$$

where $(x_{\text{PD}}, y_{\text{PD}})$ is the $(x, y)$ coordinate of the center of the PR and $h_{\text{PD}}$ is the receiver's height. The orientation of PD $i$ is defined as follows:

- The elevation angles of all PDs are equal to $\theta_{\text{PR}}$ which is a parameter to be determined. In other words, $\theta^i_{\text{PD}} = \theta_{\text{PR}}$ for $i \in \{1, \cdots, N\}$.
- The azimuth angle of the PD $i$ is given by

$$\phi^i_{\text{PD}} = \frac{2(i-1)\pi}{N}, \quad (9)$$

such that all the azimuth angles are aligned symmetrically.

These properties can be fulfilled by putting PDs on an equilateral $N$-gon based pyramid. Additionally, the horizontal orientation of the whole receiver can be varied by $\phi_{\text{PR,H}} \in [0, 2\pi)$, so that the resulting azimuth of PD $i$ is $\phi^i_{\text{PD}} + \phi_{\text{PR,H}}$. Note that $\phi_{\text{PR,H}}$ can be (i) caused by the random orientation of a receiver or (ii) purposely introduced to maximize the channel capacity. The PD placement and $\phi_{\text{PR,H}}$ of a PR on the horizontal plane with $N = 4$ and $N = 8$ are shown in Fig. 5(a) and Fig. 5(b), respectively. Optimal elevation angle $\theta^{\text{opt}}_{\text{PR}}$ and optimal horizontal orientation $\phi^{\text{opt}}_{\text{PR,H}}$ maximizing the channel capacity can be found by numerical evaluation using (7). More details will be shown in Section IV.

In a PR, the PDs are placed close to each other but their orientations can be very different. This is the key to induce different entries in the MIMO channel matrix according to (3) and hence reduce the correlation of the wireless links. The receiver does not take much space as in Fig. 6, where top and side views of a PR constructed for $N = 4$ are shown. The upper bounds on the size of the receiver are given in millimeters with the assumption that four typical off-the-shelf OSD15-E PDs are used. Due to symmetry of the PR, side views are the same.

*2) Definition of Hemispheric Receiver (HR):* Similar to PR, we are not required to put PDs on a hemisphere to build a hemispheric receiver. We just use the geometry of a hemisphere to determine the normal vectors of the PDs in a HR. To be specific, the coordinates of the PDs in a HR are the same as those in a PR given in (8) but the normal vectors of the PDs in a HR are chosen differently.

To determine the orientations of the PDs in a HR, we evenly distribute $2N$ points on a unit sphere such that the minimum distance between two points is maximized. Then we cut the sphere into one half and obtain the hemisphere. We denote the points on the hemisphere in spherical coordinates as $(\theta^i_{\text{HR}}, \phi^i_{\text{HR}})_{i=1}^N$. Then we set the elevation angles $\theta^i_{\text{PD}} = \theta^i_{\text{HR}}$ and the azimuth angles $\phi^i_{\text{PD}} = \phi^i_{\text{HR}}$ for $1 \leq i \leq N$ to form the normal vectors of the PDs in HR. However, to determine the coordinates of the $2N$ points, which are evenly distributed

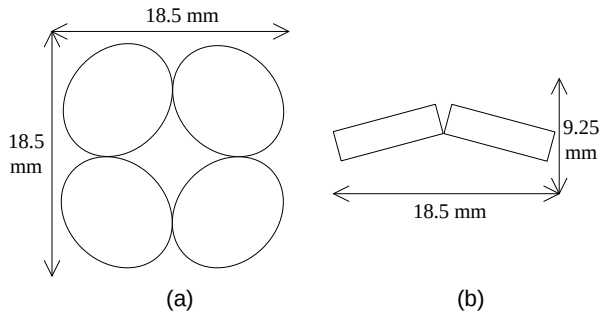


Fig. 6: PD arrangement in a PR for $N = 4$ where (a) is the top view and (b) is the side view. Due to symmetry, side views are the same. For the PDs, the normal vectors and the locations are chosen according to Fig. 3 and Fig. 5(a), respectively. Dimensions are given in millimetres for receivers constructed with typical off-the-shelf Centronic OSD15-E PDs. The actual dimension depends on the orientation of the PDs but it is always upper bounded by $18.5$ mm $\times$ $18.5$ mm $\times$ $9.25$ mm.

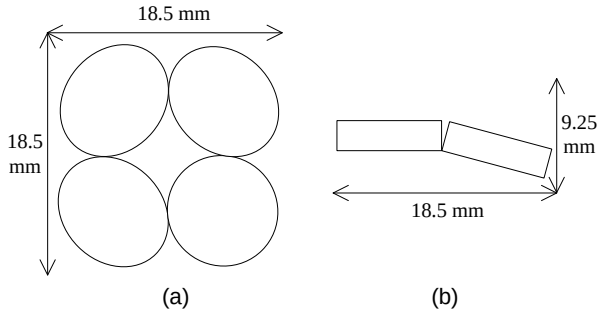


Fig. 7: PD arrangement in a HR for $N = 4$ where (a) is the top view and (b) is the side view from the right. For the PDs, the normal vectors and the locations are chosen according to Fig. 4 and Fig. 5(a), respectively. Dimensions are given in millimetres for receivers constructed with typical off-the-shelf Centronic OSD15-E PDs. The actual dimension depends on the orientation of the PDs but it is always upper bounded by $18.5$ mm $\times$ $18.5$ mm $\times$ $9.25$ mm.

on a sphere for an arbitrary $N$, is an open problem [18, 19]. Therefore, we will use the approximate solution in [20] as follows. For $1 \leq i \leq N$, we have

$$\theta_{\text{PD}}^{i} = \arccos(t_i), \tag{10}$$

and for $2 \leq i \leq N$,

$$\phi_{\text{PD}}^{i} = \left( \phi_{\text{PD}}^{i-1} + \frac{3.6}{\sqrt{2N}} \frac{1}{\sqrt{1-t_i^2}} \right) (\text{mod } 2\pi), \tag{11}$$

where $\phi_{\text{PD}}^{1} = 0$ and

$$t_i = 1 - \frac{2(i-1)}{2N-1}. \tag{12}$$

In (11), (mod $2\pi$) is used to ensure that $\phi_{\text{PD}}^{i} \in [0, 2\pi]$ for $2 \leq i \leq N$. Similar to PR, a HR could be rotated horizontally by $\phi_{\text{HR,H}} \in [0, 2\pi)$ such that the azimuth angle of the PD $i$ in HR becomes $\phi_{\text{PD}}^{i} + \phi_{\text{HR,H}}$.

Similar to PR, HR does not take much space to construct. This can be verified from Fig. 7 for HR ($N = 4$) constructed with four typical off-the-shelf OSD15-E PDs. An upper bounded on the size is given.

## III. Theoretical Evaluations

### A. Effect of Field-of-View (FoV) Coefficient of the Photodiode Receiver

In conventional wireless MIMO systems, the entries of the channel matrix are usually assumed to be independent Rayleigh random variables. However, our considered VLC-MIMO system does not have such properties. It is even natural to suspect that whether the channel matrix $\mathbf{H}$ in (2) has full rank as all the entries are deterministic according to (3).

In the following, we show a surprising fact that the rank of $\mathbf{H}$ is indeed affected by the FoV coefficient of the photodiode receiver (i.e., $k$ in (3)).

In some of the literature, the general formula for the FoV channel is given with the assumption that $k = 1$ until the FoV angle is reached (see Eqn. (3) in [11]). In our experiments as shown in Section IV, we find that $k = 1.4738$. The following theorem shows that using PDs with $k = 1$ has disadvantages in terms of the maximum number of multiplexed channels.

Consider a non-imaging receiver which consists of $N$ PDs. Suppose there are $M$ LEDs which are within the LoS of the $N$ PDs. The LED $j$ and PD $i$ are as depicted in Fig. 1. Suppose the distance between the LED $j$ and the receiver is much larger than the spatial separation (distance) between the PDs in a receiver. Then we can assume that $\alpha_j = \alpha_{ij}$ and $d_j = d_{ij}$ for all $i$ to simplify the analysis. The channel gain can be rewritten as

$$h_{ij} = \frac{(m+1)A}{2\pi d_j^2} \cos^m(\alpha_j) \cos^k(\beta_{ij}). \tag{13}$$

**Theorem 1.** *Suppose there are $M$ LEDs and $N$ PDs with $M, N \geq 3$. Assume that the channel gain is given by* (13)*. If $k = 1$, then the number of independent channels is upper bounded by 3 regardless of $M$ and $N$.*

*Proof.* Let $\mathbf{n}_i$ and $\mathbf{r}_j$ be 3-dimensional column vectors where $\mathbf{n}_i$ denotes the normal vector of PD $i$ and $\mathbf{r}_j$ denotes the vector pointing to LED $j$ from the receiver. For $1 \leq i \leq N$ and $1 \leq j \leq M$, assume $|\mathbf{n}_i| = |\mathbf{r}_j| = 1$. Then it is easy to check that $\mathbf{n}_i \cdot \mathbf{r}_j = \cos\beta_{ij}$. Let $\xi_j = \frac{(m+1)A}{2\pi d_j^2} \cos^m(\alpha_j)$. Together with $k = 1$, (13) can be rewritten as

$$h_{ij} = (\xi_j \mathbf{r}_j) \cdot \mathbf{n}_i. \tag{14}$$

Hence, the channel matrix $\mathbf{H}$ is given by

$$\mathbf{H} = F^* G, \tag{15}$$

where $F$ is a $3 \times N$ matrix with the $j$-th column equal to $\xi_j \mathbf{r}_j$ and $G$ is a $3 \times M$ matrix with the $i$-th column equal to $\mathbf{n}_i$. The capacity of a MIMO system with equal transmitted power

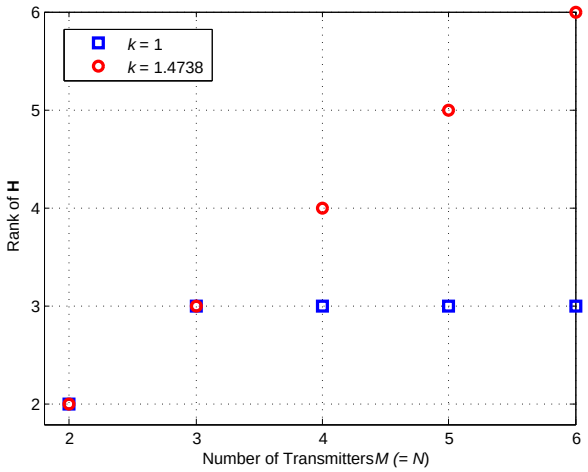


Fig. 8: The rank of channel matrix $\mathbf{H}$ for $k = 1$ and $k = 1.4738$.

is given by (7), where $\{\lambda_i\}$ are the eigenvalues of

$$W = \begin{cases} G^* F F^* G, & M \leq N, \\ F^* G G^* F, & M > N. \end{cases} \tag{16}$$

Note that both $FF^*$ and $GG^*$ are $3 \times 3$ matrices. So the rank of $W$ is upper bounded by 3 and hence, there are almost three positive eigenvalues of $W$. Therefore, the theorem is proved. □

**Example 1.** *To demonstrate how the parameter $k$ affects the rank of the channel matrix $\mathbf{H}$, we consider a VLC-MIMO system using PR. Suppose the number of LEDs is equal to the number of PDs, i.e., $M = N$. The PDs are arranged according to (8). For $1 \leq j \leq M$, the coordinates of LED $j$ are given by*

$$(x^j_{LED}, y^j_{LED}, z^j_{LED}) = \left( x_{LED} + r' \cos \frac{2(i-1)\pi}{N}, y_{LED} + r' \sin \frac{2(i-1)\pi}{N}, h_{LED} \right). \tag{17}$$

*The other parameters are specified as follows:*

- $\theta_{PR} = 40°$ *and* $\phi_{PR,H} = 45°$ *such that all LEDs are within the LoS of the PDs.*
- $x_{PD} = y_{PD} = x_{LED} = y_{LED} = 2$ *m.*
- $h_{PD} = 0.8$ *m.*
- $r = 0$ *(same as the assumption in Theorem 1).*
- $h_{LED} = 2.7$ *m.*
- $r' = 2$ *m.*

*The ranks of the channel matrix $\mathbf{H}$ for different $M = N$ are shown in Fig. 8. When $k = 1$, the rank of $\mathbf{H}$ is upper bounded by 3 as shown in Theorem 1. When $k = 1.4738$, the rank can grow linearly with $M = N$.*

### B. BER Calculation

The electrical modulation considered here is unipolar $K$-PAM as described in Section II. MIMO multiplexed channels in AWGN can be considered as parallel AWGN channels. Therefore, the theoretical BER of spatially multiplexed $M \times N$ MIMO system can be approximated as [21]:

$$\text{BER}_{\text{SM}} \simeq \frac{2(K-1)}{R_H K} \sum_{i=1}^{R_H} \mathcal{Q}\left( \sqrt{\frac{3\lambda_i \ \text{SNR}_{\text{elec}} \log_2 K}{(K-1)(2K-1)}} \right), \tag{18}$$

where $\mathcal{Q}(u) = (1/\sqrt{2\pi}) \int_u^\infty \exp(-t^2/2) dt$. This formula will be used in Section VI when we compare the performance of different MIMO systems. The above would facilitate our numerical studies.

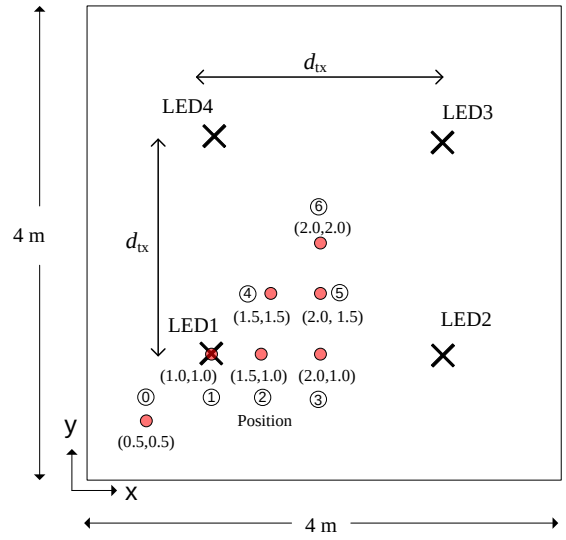


Fig. 9: The seven positions considered for performance comparison where $d_{\text{tx}} = 2$ m.

## IV. Numerical Evaluation of MIMO Channel Capacity

### A. Numerical Parameters

For the performance analysis, we will consider a space with dimensions of $4\,\text{m} \times 4\,\text{m} \times 2.7\,\text{m}$ and $M = N = i^2$ for some integers $i > 1$. The LEDs are placed in an evenly distributed square array of $\sqrt{M}$ by $\sqrt{M}$, with the center of the array coinciding with the center of the space. The length of the LED array is denoted as $d_{\text{tx}}$. The LED arrangement for $M = 4$ in the space is depicted in Fig. 9.

The following parameters are considered throughout the rest of the paper unless otherwise stated.

- We assume that all LEDs are Lambertian sources with $\Phi_{1/2} = 60°$ (which gives $m = 1$).
- All LEDs are oriented downwards, i.e., $\phi^j_{\text{LED}} = 0^o$ and $\theta^j_{\text{LED}} = 180^o$, for $1 \leq j \leq M$.
- We take $A = 15$ mm$^2$ and $k = 1.4738$ because these are the values for Centronic OSD15-E PDs [22, 23] which we used for some practical experiments in Section VII.
- The LEDs are mounted on the ceiling ($h_{\text{LED}} = 2.7$ m).
- The receivers are place at a height of 0.8 m ($h_{\text{PD}} = 0.8$ m).

- We consider $M = N = 4$ with $d_{\text{tx}} = 2$ m.

We defined $\text{SNR}_{\text{elec}}$ in (7) based on the transmitted signal power, similar to [11]. This is because we require a fair comparison of performances that encompasses the path losses of the different receivers. Due to the small PD active area, typical channel coefficients are in the order of $10^{-6}$. This results in a large path loss at the receiver, typically around 120 dB, which is around 40 dB greater than the path loss in [11]. This is because of the larger PD active area (1 $\text{cm}^2$) used in [11], compared to the smaller PD active area (15 $\text{mm}^2$) considered in this paper. Due to this reason, there is about 120 dB offset in receiver $\text{SNR}_{\text{elec}}$ with reference to the transmit $\text{SNR}_{\text{elec}}$. Therefore, unless we state otherwise we will consider $\text{SNR}_{\text{elec}} = 160$ dB in order to have reasonable performance measures because in this case, the $\text{SNR}_{\text{elec}}$ at the receiver is just about 40 dB $(= 160 - 120)$ dB.

We assume that the total transmit power from all LEDs is a constant so that (7) will be used. Furthermore, we assume that all links have direct LoS and reflections are not considered. Besides, we assume that optical filters are not used in the PD receivers.

We consider seven positions, from Positions 0 to 6, where Position 6 is at the center of the space, as depicted in Fig. 9. Due to the transmitter array symmetry, considering these seven positions would provide insights about a large area of the space.

### *B. Evaluation of the Optimum Orientation Angles of PR and HR*

As mentioned previously, we can vary the elevation angle $\theta_{\text{PR}}$ and the horizontal rotation $\phi_{\text{PR,H}}$ of the PR to find $\theta_{\text{PR}}^{\text{opt}}$ and $\phi_{\text{PR,H}}^{\text{opt}}$ that maximizes the channel capacity at each position in the space. The channel capacity variations across the seven positions at different $\theta_{\text{PR}}$ for $\phi_{\text{PR,H}} = 45°$ are shown in Fig. 10. The radius of the circle $r$ of the PD placement is set to 0.5 cm, which is the minimum $r$ according to the size of PDs used in our experiments. By varying $\theta_{\text{PR}}$ for different $\phi_{\text{PR,H}}$ values and calculating the capacity, we can find $\theta_{\text{PR}}^{\text{opt}}$ and $\phi_{\text{PR,H}}^{\text{opt}}$ for the pyramid receiver, while for the hemispheric receiver we vary $\phi_{\text{HR,H}}$ to find $\phi_{\text{HR,H}}^{\text{opt}}$. These optimal angles are reported in Table I.

TABLE I: Optimum orientation angles for PR and HR for the seven positions in the space with $M = N = 4$.

| Position | $\theta_{\text{PR}}^{\text{opt}}$ | $\phi_{\text{PR,H}}^{\text{opt}}$ | $\phi_{\text{HR,H}}^{\text{opt}}$ |
|---|---|---|---|
| 0 | 40° | 45° | 230° |
| 1 | 49° | 45° | 230° |
| 2 | 53° | 45° | 230° |
| 3 | 54° | 45° | 230° |
| 4 | 56° | 45° | 230° |
| 5 | 56° | 45° | 230° |
| 6 | 58° | 45° | 230° |

## V. MIMO Channel Capacity Comparison

We now numerically compare the channel capacities of the proposed receivers with other VLC-MIMO systems including spatially separated (SS) receiver and link-blocked (LB) receiver [11]. The SS receiver is defined as a square array of $\sqrt{N}$ by $\sqrt{N}$ PDs with each side equal to $d_{\text{SS}} = 10$ cm. For PR, HR, and LB receivers, the PDs are located on a circle with radius equal to 0.5 cm as described in Section II-C(see Fig. 5). The normal vectors of all the PDs of LB and SS receivers are set to $[x_{\text{PD}}^i, y_{\text{PD}}^i, z_{\text{PD}}^i, 0, 0]$, for $1 \leq i \leq N$. For LB receiver, the link between LED $i$ and PD $i$ is blocked so that

$$h_{ii} = 0, \quad \forall i. \tag{19}$$

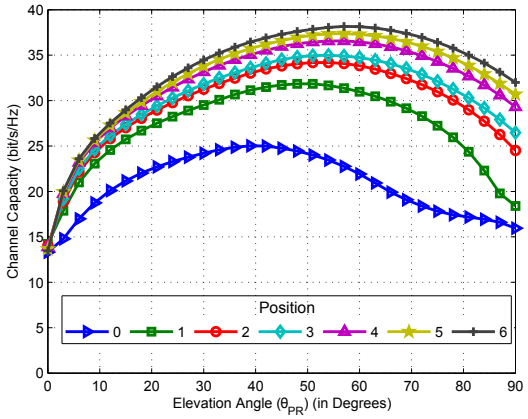


Fig. 10: Channel capacity of PR as a function of $\theta_{\text{PR}}$ for $\phi_{\text{PR,H}} = 45°$ across the seven positions of the space.

For the PR, we fix $\theta_{\text{PR}} = 56°$ as it provides a compromise among the optimal values at or near the center of the space, where we assume the user will use VLC mostly. Also we fix $\phi_{\text{PR,H}} = 45°$ as this is the optimal horizontal orientation angle found for all the positions. At the center of the space the channel matrix for PR, denoted by $\mathbf{H}_{\text{PR}}$, is

$$\mathbf{H}_{\text{PR}} = 10^{-6} \begin{pmatrix} 0 & 0.2083 & 0.6285 & 0.2083 \\ 0.2083 & 0 & 0.2083 & 0.6285 \\ 0.6285 & 0.2083 & 0 & 0.2083 \\ 0.2083 & 0.6285 & 0.2083 & 0 \end{pmatrix}. \tag{20}$$

The eigenvalues of $\mathbf{H}_{\text{PR}}\mathbf{H}_{\text{PR}}^*$ are $4.5 \times 10^{-14}$, $3.95 \times 10^{-13}$, $3.95 \times 10^{-13}$ and $1.092 \times 10^{-12}$.

For HR, we fix $\phi_{\text{HR,H}}$ at 230°, which is the optimal horizontal orientation angle for all the positions of the space. At the center of the space the channel matrix for HR, denoted by $\mathbf{H}_{\text{HR}}$, is

$$\mathbf{H}_{\text{HR}} = 10^{-6} \begin{pmatrix} 0.4961 & 0.4936 & 0.4906 & 0.4931 \\ 0.1995 & 0.6526 & 0.4115 & 0.0529 \\ 0 & 0.0879 & 0.5623 & 0.2001 \\ 0.0075 & 0 & 0.0538 & 0.4057 \end{pmatrix}. \tag{21}$$

The eigenvalues of $\mathbf{H}_{\text{HR}}\mathbf{H}_{\text{HR}}^*$ are $3 \times 10^{-14}$, $1.5 \times 10^{-13}$, $2.48 \times 10^{-13}$ and $1.713 \times 10^{-12}$.

**Remarks:** It can be checked that the number of positive eigenvalues for both $\mathbf{H}_{\text{PR}}$ and $\mathbf{H}_{\text{HR}}$ are equal to 4. In fact, among the 210 points in Fig. 10, the ranks of $\mathbf{H}_{\text{PR}}$ are equal to 4 for 203 points and 3 for 7 points.

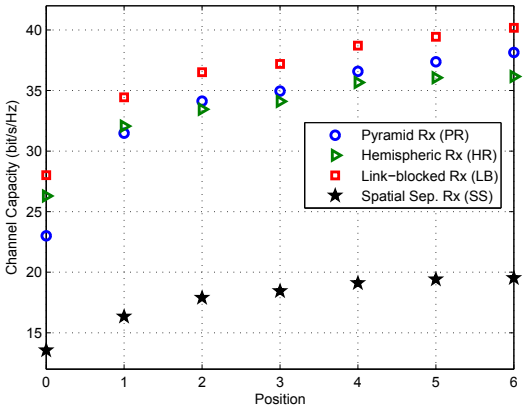


Fig. 11: Channel capacity of the PR, HR, LB and SS receivers across the seven positions of the space.

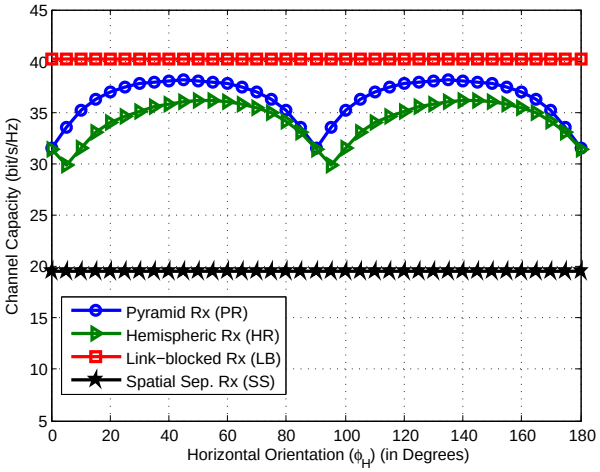


Fig. 12: Channel capacity as a function of horizontal orientation ($\phi_{\text{H}}$) of the PR, HR, LB and SS receivers at Position 6.

### *A. Varying the position of the receiver*

We now consider the different receiver designs at different positions of the space. Channel capacity variation of the PR, HR, LB and SS receivers across the seven positions of the space is depicted in Fig. 11. It is shown that LB has the highest capacity compared to the other three receivers. However, it should be noted that the physical structure of the LB receiver needs to be adjusted at each position to achieve the induced link blockage in (19) while the other three receivers do not need any adjustment from position to position.

Note that overall the PR is better than the HR in the achievable capacity except at Positions 0 and 1. The main reason for PR performing worse than HR at these two positions is the selection of the fixed angle values ($\theta_{\text{PD}}$ and $\phi_{\text{PR,H}}$) for the PR which are not the optimal values that gives the best performance when the receiver is placed near the corners of the space, whereas the fixed horizontal angle of HR ($\phi_{\text{HR,H}}$) is optimal throughout the space (see Table I).

### *B. Varying the horizontal orientation of the receiver*

By varying the horizontal orientation angle ($\phi_{\text{H}}$) of the receivers, the variation in channel capacity for the receiver located at the center of the space is depicted in Fig. 12. At the center of the space, the horizontal rotation for PR and HR are symmetric for every $45°$ and $90°$, respectively, due to the symmetric orientations of LEDs. Therefore, it is sufficient to consider only $180°$ in Fig. 12. The proposed receivers are sensitive to changes in horizontal rotation. The maximum and the minimum channel capacities of the HR are slightly lower than the respective channel capacities of the PR generally. Comparing with SS, PR and HR show larger capacities for all $\phi_{\text{H}}$.

### *C. Varying the length of the LED transmitter array*

We now vary the length $d_{\text{tx}}$ of the LED transmitter array. The result is shown in Fig. 13.

The channel capacity of LB receiver shows a relatively fast decrease with the increase of $d_{\text{tx}}$. For the other three receivers, the channel capacity first increases and then decreases so that there exists an optimal $d_{\text{tx}}$ for the maximum capacity.

The capacity decrease in LB with increasing $d_{\text{tx}}$ is due to the decrease of received signal power caused by the increase of the distance between the transmitters and receivers. For the SS receiver, increasing $d_{\text{tx}}$ initially enhances the channel capacity due to the consequence of channel de-correlation which compensates the loss of the received signal strength. Until a certain $d_{\text{tx}}$ is reached, the channel capacity is maximized. However, a further increase of $d_{\text{tx}}$ from this value would make the received signal power decrease more prominent compared to the benefit of reduced channel correlation. The two proposed receivers PR and HR also show similar characteristics.

However, it is worth noting that the channel capacities of PR and HR become greater than that of LB at some points, after around $d_{\text{tx}} = 2.25$ m and $d_{\text{tx}} = 3$ m, respectively. This is due to the following reason. Note that the PDs in PR and HR are inclined but the normal vectors of PDs in SS and LB are always vertical. When the LEDs are far away from each other with large $d_{\text{tx}}$, there still exists a PD in PR (or HR) which enjoys smaller incident angle compared with the PDs in SS and LB. Generally speaking, in comparison to SS, the channel capacities of PR and HR are always higher for different $d_{\text{tx}}$.

### *D. Varying the number of transmitters/receivers* $(M = N)$

We now vary the number of LED transmitters and PD receivers for $M = N = i^2$ where $i = 2, 3, 4$ and 5, and find the minimum $\text{SNR}_{\text{elec}}$ required to achieve a channel capacity of 40 bits/s/Hz. Placements of the LEDs are done according to the description given in Section IV-A. The receivers are always placed at the center of the space (i.e., Position 6). By using a similar approach as done in Section IV-B, we can find $\theta_{\text{PR}}^{\text{opt}}$ and $\phi_{\text{PR,H}}^{\text{opt}}$ for the PR and $\phi_{\text{HR,H}}^{\text{opt}}$ for the HR, for different number of PD receivers placed at Position 6. The results are summarized in Table II. The PR becomes less sensitive to $\phi_{\text{PR,H}}$ rotation as the number of PD receivers increases because the system becomes the same if the receiver is rotated by $\frac{360}{N}°$ (cf. Fig. 5).

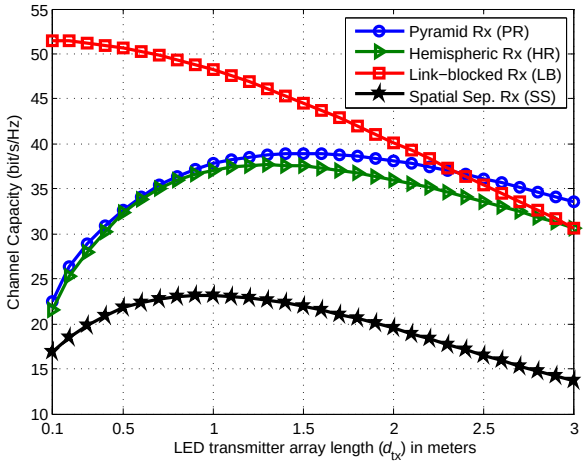


Fig. 13: Channel capacity as a function of the separation distance between LEDs ($d_{\text{tx}}$) for the PR, HR, LB and SS receivers located at Position 6.

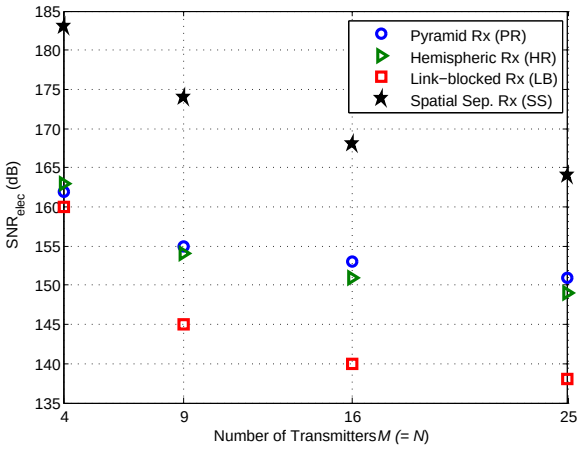


Fig. 14: $\text{SNR}_{\text{elec}}$ required to achieve a channel capacity of 40 bits/s/Hz for $M = N = 4, 9, 16$ and 25 of PR, HR, LB and SS receivers at Position 6.

On the other hand, $\theta_{\text{PR}}^{\text{opt}}$ increases with $M = N$. For a large $M$, a large number of LEDs are closely packed. A larger $\theta_{\text{PR}}^{\text{opt}}$ reduces the channel correlation by reducing the numbers of LEDs within the field of view of each PD. This compensates the loss of signal strength due to a large incident angle.

The minimum $\text{SNR}_{\text{elec}}$ required to achieve a channel capacity of 40 bits/s/Hz is shown in Fig. 14, for PR, HR, LB and SS. To obtain the results in Fig. 14, we have used the optimal values shown in Table II. In Fig. 14, LB receiver outperforms the other three receivers. The SS receiver has the worst performance.

### *E. Spatial Separation Variation*

We have seen so far that the proposed receivers, PR and HR outperform SS receiver in the capacity comparison, where the SS receiver is confined to have fixed spatial separation of $d_{\text{SS}} = 10$ cm. However, it is fairer to compare by allowing different spatial separation. In the following, we consider $M = N = 4$ and increase the spatial separation of the PDs in SS receiver until it can achieve same capacity as PR and HR. The minimum spatial separation of the SS receiver, $d_{\text{SS}}^{\text{min}}$ for achieving same capacity is shown in Table III. From Table III, we can see that the SS receiver requires the separation between the PDs from 38 cm to 131 cm in to achieve the same capacity as the proposed PR and HR. In practice, it would be difficult to use SS receiver for achieving same capacity of PR or HR to be placed in small hand-held devices.

TABLE II: Optimum orientation angles for PR and HR for different number of transmitters $M(= N) = 4, 9, 16$ and 25 placed at the center of the space (i.e., Position 6).

| Number of transmitters $M(= N)$ | $\theta_{\text{PR}}^{\text{opt}}$ | $\phi_{\text{PR,H}}^{\text{opt}}$ | $\phi_{\text{HR,H}}^{\text{opt}}$ |
|---|---|---|---|
| 4 | 56° | 45° | 230° |
| 9 | 66° | 20° | 260° |
| 16 | 69° | 0° | 215° |
| 25 | 73° | 0° | 230° |

## VI. BER Comparisons

We now compare the BER performance of the optical wireless MIMO systems for 4-PAM modulation with $M = N = 4$.

### *A. Varying the position of the receiver and the length of the LED transmitter array*

Simulated and analytical BER performance are shown in Fig. 15 and Fig. 16 for the receivers placed at Position 0 and Position 6 (i.e., the center of the space), respectively. In both cases, $d_{\text{tx}} = 2$ m.

We can see that the theoretical results closely match the simulated results for high $\text{SNR}_{\text{elec}}$ for all the systems. SS receiver has much poorer BER performance compared to the other receivers in both positions due to the higher channel correlation. LB receiver shows the best BER performance. For a BER of $10^{-4}$, the $\text{SNR}_{\text{elec}}$ improvement of the LB receiver compared to PR are 7 dB and 4 dB, for receiver at Position 0 and Position 6, respectively. Compared with HR, LB receivers shows $\text{SNR}_{\text{elec}}$ improvement of 4 dB and 7 dB for receiver at Position 0 and Position 6, respectively. The better performance of LB receiver shows that link blocking is a better way to overcome channel correlation. However, it needs to pay the

TABLE III: Minimum spatial separation required for SS receiver ($d_{\text{SS}}^{\text{min}}$) to achieve the same capacity as PR and HR.

| Position | $d_{\text{SS}}^{\text{min}}$ to achieve PR channel capacity | $d_{\text{SS}}^{\text{min}}$ to achieve HR channel capacity |
|---|---|---|
| 0 | 0.85 m | 1.31 m |
| 1 | 0.75 m | 0.81 m |
| 2 | 0.64 m | 0.62 m |
| 3 | 0.61 m | 0.56 m |
| 4 | 0.52 m | 0.48 m |
| 5 | 0.49 m | 0.43 m |
| 6 | 0.45 m | 0.38 m |

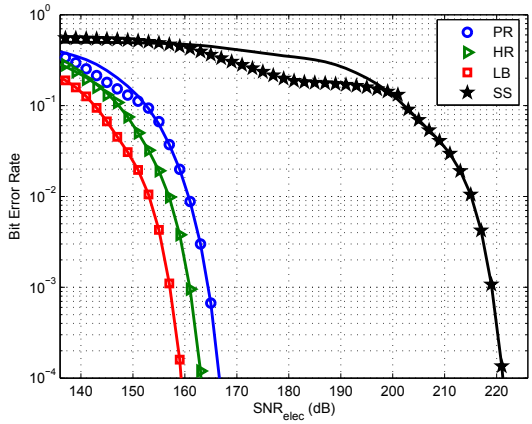


Fig. 15: BER as a function of $\text{SNR}_{\text{elec}}$ of the PR, HR, LB and SS receivers at Position 0 with simulation curves (lines) and analytical curves (markers) for $d_{\text{tx}} = 2$ m.

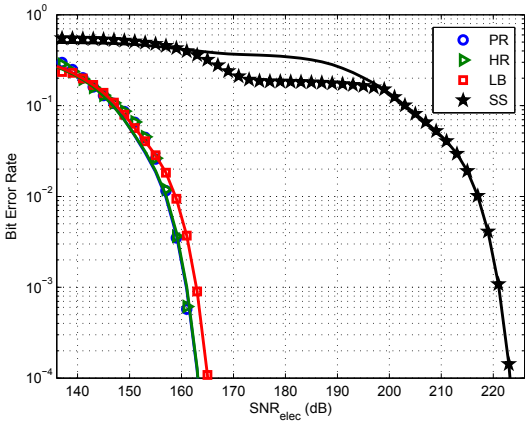


Fig. 17: BER as a function of $\text{SNR}_{\text{elec}}$ of the PR, HR, LB and SS receivers at Position 0 with simulation curves (lines) and analytical curves (markers) for $d_{\text{tx}} = 3$ m.

price for adjusting the receiver designs at different positions. The PR performs better than HR, in terms of BER at Position 6 (at the center), while HR outperforms PR at Position 0. This is due to the optimality of the fixed construction of HR for both positions which in comparison to PR, which is optimized to perform better near the center of the space.

We will now increase the distances between the LEDs, $d_{\text{tx}}$, from 2 m to 3 m. The results are shown in Fig. 17 and Fig. 18 for the receivers placed at Position 0 and Position 6, respectively. Similar to the case of channel capacity (see Fig. 13 at $d_{\text{tx}} = 3$ m), the PR outperforms the other three receivers in BER at the center of the space where PR has 2 dB and 6.5 dB advantage in $\text{SNR}_{\text{elec}}$ compared to the LB receiver and HR, respectively. At Position 0, BER performance of PR and HR are almost the same and both outperform LB and SS receivers. At Position 0, PR and HR have 2 dB advantage in $\text{SNR}_{\text{elec}}$ compared to LB receiver for BER $= 10^{-4}$. The $\text{SNR}_{\text{elec}}$ degradation of the LB receiver is due to the loss in received power because of the larger distance $(d_{\text{tx}})$ between the receivers and transmitters compared to the case of Fig. 16. PR and HR both improve their performances compared to LB receiver when $d_{\text{tx}} = 3$, due to the angle inclination of the PDs that can reduce the channel correlation as well as keep the received power at an acceptable level.

It is clear that SS receiver is worse than the other three receiver designs generally.

### *B. Rotation of the receiver*

The proposed PR and HR receivers are suitable to be used in hand-held devices, where the user can arbitrarily change the orientation of the device. Therefore, to simulate this effect, the normal vectors of the receivers are rotated around x- and z- axes by rotation matrices, $\mathbf{R_x}(\theta)$ and $\mathbf{R_z}(\phi)$, respectively, where $0° \leq \theta \leq 90°$ and $0° \leq \phi \leq 359°$ as defined in Section II-B. Consider any fixed $\theta$. We first rotate the normal vectors of the receivers around z-axis by $\phi$ and then rotate it around x-axis by $\theta$.

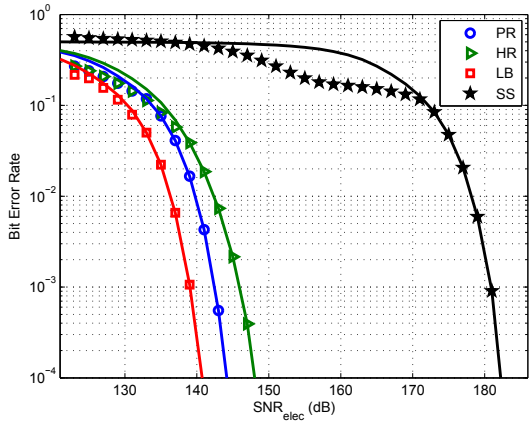


Fig. 16: BER as a function of $\text{SNR}_{\text{elec}}$ of the PR, HR, LB and SS receivers at Position 6 with simulation curves (lines) and analytical curves (markers) for $d_{\text{tx}} = 2$ m.

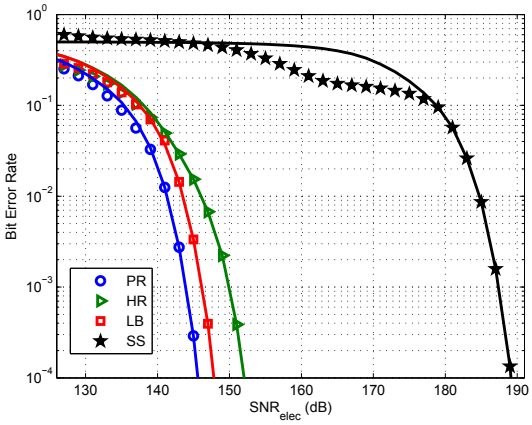


Fig. 18: BER as a function of $\text{SNR}_{\text{elec}}$ of the PR, HR, LB and SS receivers at Position 6 with simulation curves (lines) and analytical curves (markers) for $d_{\text{tx}} = 3$ m.

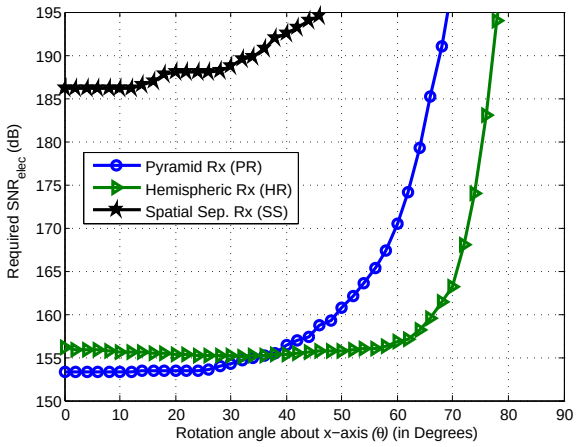


Fig. 19: Average $\text{SNR}_{\text{elec}}$ required to achieve a BER of $10^{-4}$ as a function of rotation angle about x-axis ($\theta$) of the PR, HR and SS receivers at Position 6.

We numerically evaluate the average $\text{SNR}_{\text{elec}}$ required to achieve a BER of $10^{-4}$ for different $\theta$ with $\phi$ having a uniform distribution. The respective performances of PR, HR and SS receivers placed at the center of the space for different $\theta$ values are depicted in Fig. 19. BER performances of all three receivers become worse for large $\theta$. HR is the most robust of the three receivers for rotations because the normal vectors of its PDs are oriented non-symmetrically and hence can achieve lower correlation as well as receive higher incident power for a larger $\theta$, compared to the PR and SS. It is clear that SS receiver performs the worst. We have not considered the LB receiver in this section as it is not practical, especially in this case.

## VII. Experimental Results

We now show experimental results to verify the feasibility of our proposed PR in a $4 \times 4$ MIMO system. Four Bridgelux

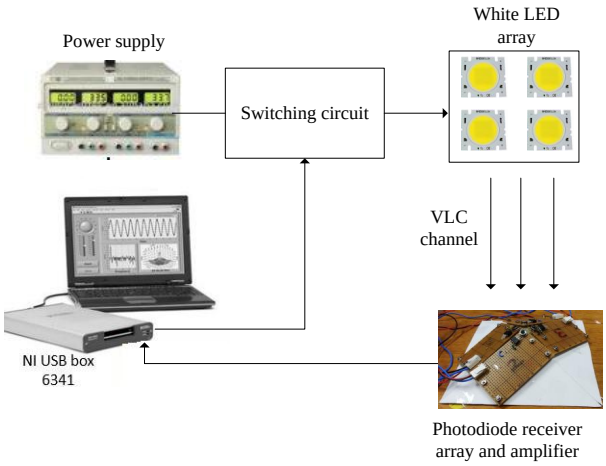


Fig. 20: Experimental setup.

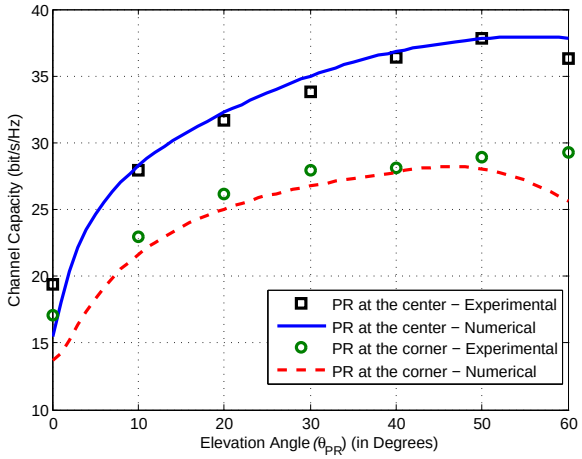


Fig. 21: Experimental and numerical results for PR with varying $\theta_{\text{PD}}$ for the receiver placed at the center of the LED array and at the corner of the room.

BXRA-50C5300 white LEDs [24] are arranged in an array of $2 \times 2$ and are placed in coordinates (in meters) equal to $(1.1, 0.9, 2.7), (2.4, 0.9, 2.7), (2.4, 1.8, 2.7)$ and $(1.1, 1.8, 2.7)$. The LEDs are switched by a power electronic circuit based on MOSFETs, which is controlled by a personal computer through a data acquisition device (DAQ of National Instrument USB-6341 X Series). We use Centronic OSD15-E PDs [22] as the receivers and the receive signals from the PDs are amplified by an operational amplifier circuit before the signals are fed to the DAQ. The electrical modulation used is 2-PAM. The experimental setup is depicted in Fig. 20.

The $4 \times 4$ MIMO experimental parameters are the same as those used for the numerical evaluation in Section IV. We send a pilot data sequence to the PDs through the visible light channel from the LEDs. Based on the data input to the PC from the PDs, we calculate the channel coefficients and evaluate the

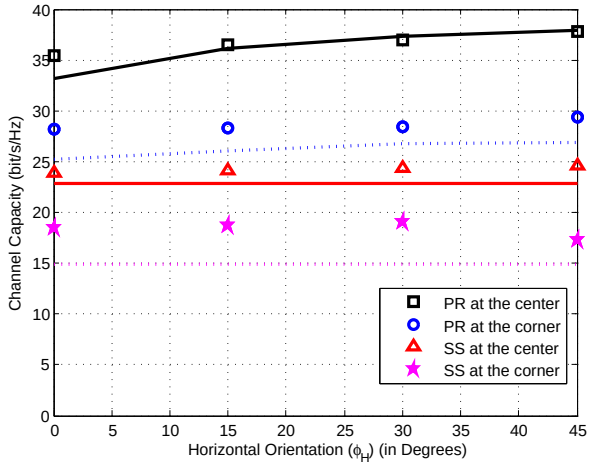


Fig. 22: Experimental (markers) and numerical (lines) graphs for PR and SS with varying horizontal orientation for receivers placed at the center of the LED array and at the corner of the room.

capacity using (7). The experimental and the numerical results for the proposed PR at different elevation angles $\theta_{\text{PR}}$ ranging from $0^\circ$ to $60^\circ$ (fixed $\phi_{\text{PR,H}} = 45^\circ$), when receiver placed at coordinates (1.75, 1.35, 0.8) which is the center of the LED array, and at the corner of the room on at coordinates (0.5, 0.5, 0.8) are shown in Fig. 21. As we can see, the experimental and numerical results are well matched.

In Fig. 22, we investigate the capacity with respect to the horizontal rotation of the PD array. The proposed PR with $\theta_{\text{PR}} = 50^\circ$ is compared with the SS receiver with $10$ cm spacing between adjacent PDs. The experimental and numerical results for the PR at both locations and the SS receiver at the center show an acceptable match although the experimental result from the SS receiver located at the corner, deviates from the numerical result. This can be due to the visible light reflection from the walls, which has not been considered in our analysis. The reflection is more prominent at the corner of the room. As SS receiver has PDs lying flat, all of them can easily receive the reflected lights. Therefore, the experimental result shows a channel capacity larger than that of numerical result for the SS receiver.

## VIII. Future Work and Discussion

In this paper, we have proposed two designs of angle diversity receivers which can achieve high multiplexing gains in MIMO VLC channels. It is interesting to investigate a receiver design which can also improve the coverage of the receiver. Due to the limited space, this will be left as future work. Furthermore, the effects of optical filters and the FoV coefficients of PD receivers are yet to be considered in the future. To keep the analytical part tractable, we have not considered reflections from the walls and ceilings of the room. However, our experimental results showed that there is a significant incident power on the PD receivers from the reflections, especially at the corner of the room. Therefore, analytical results involving reflection should be an important future work.

## IX. Conclusion

We have presented two receiver designs, namely pyramid receiver (PR) and hemispheric receiver (HR), for indoor MIMO visible light communications systems to achieve multiplexing gain. The proposed receivers support mobile users and additionally they do not occupy much space so that they are suitable for hand-held devices. Numerical evaluation of the channel capacities and the analytical and simulated BER, is carried out for a $4 \times 4$ MIMO system in an indoor space to compare the performance of the proposed angle diversity receivers with spatially separated (SS) and link-blocked (LB) receivers. Comprehensive performance comparisons are conducted for different locations in the space, different separation distances between the LED transmitters, and different horizontal orientations of the receiver array. The channel capacity and BER performance under different numbers of transmitters and receivers are also reported.

It is clear that the proposed receivers perform much better than the spatially separated PD array. Compared with the link-blocked receiver, the proposed pyramid receiver is better when the LED separation is large.

We conclude that the two proposed receiver designs are practical solutions to enable parallel data transmission in VLC-MIMO. They are attractive for their small size and do not have a requirement of spatial separation for diversity gain. As a result, they are small enough to be applicable in hand-held devices. In contrast to link-blocked receiver, the two proposed receiver designs do not require any hardware adjustment for different receiver locations so that they are also suitable for applications requiring high mobility. Meanwhile, their channel capacity and BER performance are close to that of the LB receiver. Our study also clearly shows that our proposed PR and HR are much more promising than SS receiver. We therefore believe that angle diversity receivers, particularly PR and HR, will play a significant role and have very high potential in future MIMO visible light communication systems.

## X. Acknowledgement

The authors would like to express their gratitude to the anonymous reviewers and the editors for valuable comments and suggestions that enhanced the quality of the paper.

## References

[1] F. R. Gfeller and U. Bapst, "Wireless in-house data communication via diffuse infrared radiation," *Proceedings of the IEEE*, vol. 67, no. 11, pp. 1474–1486, Nov 1979.

[2] L. Hanzo, H. Haas, S. Imre, D. O'brien, M. Rupp, and L. Gyongyosi, "Wireless myths, realities, and futures: From 3G/4G to optical and quantum wireless," *Proceedings of the IEEE*, pp. 1853–1888, May 2012.

[3] H. Elgala, R. Mesleh, and H. Haas, "Indoor optical wireless communication: Potential and state-of-the-art," *IEEE Commun. Mag.*, vol. 49, no. 9, pp. 56–62, Sept. 2011.

[4] D. Tsonev, S. Sinanovic, and H. Haas, "Practical MIMO capacity for indoor optical wireless communication with white LEDs," in *IEEE VTC Spring*, 2013, pp. 1–5.

[5] A. Burton, Z. Ghassemlooy, S. Rajbhandari, and S.-K. Liaw, "Design and analysis of an angular-segmented full-mobility visible light communications receiver," *Trans. on Emerging Telecommun. Tech.*, Mar. 2014.

[6] S. Arnon, J. Barry, G. Karagiannidis, R. Schober, and M. Uysal, *Advanced Optical Wireless Communication Systems*. Cambridge University Press, July 2012.

[7] D. O'brien, "Visible light communications: Challenges and potential," in *Proc. IEEE Photonics Conf.*, 2011, pp. 365–366.

[8] L. Zeng, D. O'brien, H. Minh, G. Faulkner, K. Lee, D. Jung, Y. Oh, and E. T. Won, "High data rate multiple input multiple output (MIMO) optical wireless communications using white LED lighting," *IEEE Journal on Selected Areas in Communications*, vol. 27, no. 9, pp. 1654–1662, December 2009.

[9] F. Bohagen, P. Orten, and G. Oien, "Design of optimal high-rank line-of-sight MIMO channels," *IEEE Trans. on Wireless Communications*, vol. 6, pp. 1420–1425, April 2007.

[10] I. Sarris and A. Nix, "Design and performance assessment of high-capacity MIMO architectures in the presence of a line-of-sight component," *IEEE Trans. on Vehicular Tech.*, vol. 56, pp. 2194–2202, July 2007.

[11] T. Fath and H. Haas, "Performance comparison of MIMO techniques for optical wireless communications in indoor environments," *IEEE Trans. on Communications*, vol. 61, pp. 733–742, Feb. 2013.

[12] K. D. Dambul, D. O'Brien, and G. Faulkner, "Indoor optical wireless MIMO system with an imaging receiver," *IEEE Photonics Technology Letters*, vol. 23, pp. 97–99, 2011.

[13] J. B. Carruthers and J. M. Kahn, "Angle diversity for nondirected wireless infrared communication," *IEEE Trans. on Communications*, vol. 48, pp. 960–969, 2000.

[14] A. Nuwanpriya, S.-W. Ho, and C. S. Chen, "Angle diversity receiver for indoor MIMO visible light communications," in *Proc. IEEE Globecom Workshops (Optical Wireless Communications)*, 2014, pp. 529–534.
[15] J. Armstrong and B. J. C. Schmidt, "Comparison of asymmetrically clipped optical OFDM and DC-Biased optical OFDM in AWGN," *IEEE Communications Letters*, vol. 12, pp. 343–345, 2008.
[16] S.-H. Yang, E.-M. Jung, and S.-K. Han, "Indoor location estimation based on LED visible light communication using multiple optical receivers," *IEEE Comm. Letters*, vol. 17, pp. 1834–1837, Sep. 2013.
[17] A. Goldsmith, *Wireless Communications*. Cambridge University Press, 2005.
[18] E. B. Saff and A. B. J. Kuijlaars, "Distributing many points on the sphere," *Mathematical Intelligencer*, vol. 19, no. 1, pp. 5–11, 1997.
[19] L. Lovisolo and E. A. B. Da Silva, "Uniform distribution of points on a hyper-sphere with applications to vector bit-plane encoding," *IEE Proceedings - Vision, Image and Signal Processing*, vol. 148, no. 3, pp. 187–193, June 2001.
[20] E. A. Rakhmanov, E. B. Saff, and Y. M. Zhou, "Minimal discrete energy on the sphere," *Mathematical Research Letters*, vol. 1, pp. 647–662, 1994.
[21] J. G. Proakis, *Digital Communications*, 5th ed. McGraw-Hill, 2008.
[22] *OSD15-E*, Centronic. [Online]. Available: http://www.centronic.co.uk/downloads/EO%20Series%20E.pdf
[23] S.-W. Ho, J. Duan, and C. S. Chen, "Location-based information transmission systems using visible light communications," *Transactions on Emerging Telecommunications Technologies*, 2015.
[24] *RS Array Series*, Bridgelux. [Online]. Available: http://www.leds.de/out/media/Bridgelux.pdf

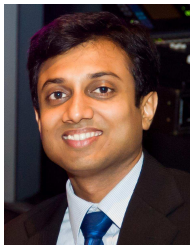

**Asanka Nuwanpriya** (S'12) received the B.Sc. in engineering with the first class honours, specialized in electronics and telecommunications, from University of Moratuwa, Sri Lanka in 2009.

From 2009 to 2011, he worked as a telecommunications engineer in leading telecommunications operators in Sri Lanka. Since 2011, he has been a Ph.D. student at the Institute for Telecommunications Research (ITR) in University of South Australia, Adelaide, Australia. His research interest include visible light communications, optical wireless communications, single-carrier communications and multi-carrier communications (OFDM) and multiple-input multiple-output (MIMO) communications.

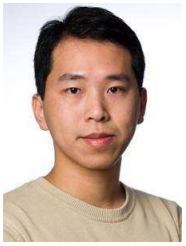

**Siu-Wai Ho** (S'05–M'07–SM'15) received the B.Eng., M.Phil., and Ph.D. degrees in information engineering from The Chinese University of Hong Kong in 2000, 2003, and 2006, respectively.

During 2006–2008, he was a Postdoctoral Research Fellow in the Department of Electrical Engineering, Princeton University, Princeton, NJ. Since 2009, he has been with the Institute for Telecommunications Research (ITR) in University of South Australia (UniSA), Adelaide, Australia, where he is now a senior research fellow. His current research interests include Shannon theory, visible light communications, information-theoretic security, and biometric security systems.

Dr. Ho was a recipient of the Croucher Foundation Fellowship for 2006–2008, the 2008 Young Scientist Award from the Hong Kong Institution of Science, UniSA Research SA Fellowship for 2010–2013, and the Australian Research Council Australian Postdoctoral Fellowship for 2010–2013.

**Chung Shue Chen** (S'02-M'05) received the B.Eng., M.Phil., and Ph.D. degrees in information engineering from the Chinese University of Hong Kong, Shatin, in 1999, 2001, and 2005, respectively.

He is a Member of Technical Staff (MTS) at Alcatel-Lucent Bell Labs. Prior to joining Bell Labs, he worked at INRIA, the French National Institute for Research in Computer Science and Control, in the research group on Network Theory and Communications (TREC, INRIA-ENS). He was an Assistant Professor at the Chinese University of Hong Kong. He was an ERCIM Fellow at the Norwegian University of Science and Technology (NTNU), Norway, and the National Center for Mathematics and Computer Science (CWI), the Netherlands.

His research interests include wireless communications and networking, radio resource management, self-organizing networks, and optimization algorithms. He has served as TPC in international conferences including IEEE ICC, Globecom, WCNC, VTC, CCNC, WiOpt, INFOCOM Workshop on Mobile Cloud and Virtualization, etc. He is an Editor of Transactions on Emerging Telecommunications Technologies (ETT) since 2011. He also holds a position of permanent member at Laboratory of Information, Networking and Communication Sciences (LINCS) in Paris. He was the recipient of Sir Edward Youde Memorial Fellowship and ERCIM Alain Bensoussan Fellowship. He was listed in Marquis Who's Who in the World (32nd Edition).